

Transient dynamics in magnetic force microscopy for a single-spin measurement

G. P. Berman,¹ F. Borgonovi,² G. V. López,³ and V. I. Tsifrinovich⁴

¹Theoretical Division and CNLS, Los Alamos National Laboratory, Los Alamos, New Mexico 87545, USA

²Dipartimento di Matematica e Fisica, Università Cattolica, via Musei 41, 25121 Brescia, Italy; INFN, Unità di Brescia, 25121 Brescia, Italy; and INFN, Sezione di Pavia, 27100 Pavia, Italy

³Departamento de Física de la Universidad de Guadalajara S.R. 500, 44420 Guadalajara, Jalisco, Mexico

⁴IDS Department, Polytechnic University, Six Metrotech Center, Brooklyn, New York 11201, USA

(Received 9 September 2002; published 9 July 2003)

We analyze a single-spin measurement using a transient process in magnetic force microscopy which could increase the maximum operating temperature by a factor of Q (the quality factor of the cantilever) in comparison with the static Stern-Gerlach effect. We obtain an exact solution of the master equation, which confirms this result. We also discuss the conditions required to create a macroscopic quantum superposition in the cantilever.

DOI: 10.1103/PhysRevA.68.012102

PACS number(s): 03.65.Ta, 03.67.Lx, 76.60.-k

I. INTRODUCTION

A magnetic force microscopy (MFM) normally studies the magnetic stray field near the sample surface. The deflection of the cantilever with the ferromagnetic tip measures a magnetic force produced by the atomic spins of the sample. The MFM resolution below 50 nm allows one to study the magnetic domains in the high-density magnetic recording media.

The routine MFM seems to be of a little use for a single-spin detection in solids. Even for unrealistically small distances between the ferromagnetic particle on the cantilever tip and the spin, the maximum temperature for a single-spin measurement comes to a millikelvin region [1]. That is why the single-spin magnetic measurement is expected to come from magnetic-resonance force microscopy (MRFM) technique [2–4].

This paper is outside the mainstream of the magnetic single-spin measurement, based on MRFM. We show the opportunity of significant increase of the MFM sensitivity, which may transfer the MFM single-spin measurement from a “gedanken experiment” to a realistic proposal.

In this paper, we show that using a transient process, one can increase the maximum temperature of a single-spin measurement by a factor of Q (the quality factor of the cantilever). Alternatively, one can increase the distance between the ferromagnetic particle and the cantilever tip if one is willing to work at millikelvin temperatures. In Sec. II, we explain the basic idea of our work. In Secs. III–IV, we obtain an exact solution of the master equations, which confirms our idea. In Sec. VI, we derive the conditions for creating a macroscopic quantum superposition in MFM. In Conclusion, we summarize our results.

II. TRANSIENT PROCESS IN MFM

In this section, we describe the basic idea of our work. Suppose that a ferromagnetic particle on the cantilever tip interacts with a single spin on the solid surface. (See Fig. 1.) The equilibrium position of the cantilever tip depends on the spin direction. The distance between two possible equilib-

rium positions, corresponding to two spin stationary states, is given by $2F/k_c$, where k_c is the cantilever spring constant, F is the magnetostatic force between the ferromagnetic particle and the spin. In order to measure the state of the spin, this distance must be greater than twice the uncertainty due to the thermodynamical noise of the cantilever position. This uncertainty can be estimated as $(k_B T/k_c)^{1/2}$, where k_B is Boltzmann’s constant and T is the temperature. Thus, the condition for a single-spin measurement (the static Stern-Gerlach effect) is [1]

$$T < T_{max} = F^2/k_B k_c. \quad (1)$$

Now, assume that we quickly change the stationary state of the spin and consider the transient cantilever vibrations after this change. The amplitude of the cantilever vibrations at time $t \ll Q/\omega_c$ (ω_c is the cantilever frequency and Q/ω_c is the time constant of the cantilever) is $4F/k_c$. In addition, assume that we detect the position and momentum of a point on the cantilever tip with an accuracy that satisfies the quantum limit $(\delta P_z)(\delta Z) \approx \hbar/2$ (the cantilever oscillates along the z axis.) To find out the state of the spin, we are going to compare the observed trajectory of the cantilever tip with the

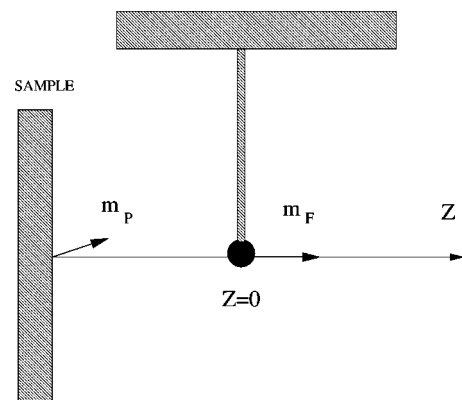


FIG. 1. Geometry of the proposed gedanken experiment. \mathbf{m}_F and \mathbf{m}_p are the magnetic moments of the ferromagnetic particle and paramagnetic atom.

theoretical prediction. The theory predicts the cantilever trajectory within an uncertainty due to the thermal noise. However, the thermal uncertainty of the cantilever position at time $t \ll Q/\omega_c$ increases as $[t(\omega_c/Q)(k_B T/k_c)]^{1/2}$. We can obtain this expression assuming an initial ($t \ll Q/\omega_c$) thermal diffusion with two common properties: (1) The dispersion $(\delta Z)^2$ is proportional to time t and (2) the uncertainty of the cantilever position equals its thermodynamical value if we formally put $t = Q/\omega_c$.

At the time $t = \pi/\omega_c$ (half of the first period), the distance between two possible cantilever positions takes its maximum possible value $4F/k_c$. At the same time, the thermal uncertainty of the position predicted by the theory is still much smaller than its thermodynamical value. Now, the condition for a single-spin measurement is

$$T < T_{max} = \frac{4QF^2}{\pi k_B k_c}. \quad (2)$$

One can see that the maximum temperature for a single-spin measurement increases by a factor of Q , compared with the static Stern-Gerlach effect. In the next three sections, we will confirm this estimation by a direct solution of the master equation.

III. THE HAMILTONIAN AND THE MASTER EQUATION

We assume that the cantilever tip with an attached ferromagnetic particle can oscillate along the z axis. (See Fig. 1.) A single paramagnetic atom with spin $\frac{1}{2}$ is placed near the cantilever tip. The dimensionless Hamiltonian of the cantilever tip interacting with a single spin is

$$\hat{H} = \frac{1}{2}(\hat{p}_z^2 + \hat{z}^2) - 2\eta \hat{z} \hat{S}_z. \quad (3)$$

We introduced the following notations (below we omit hats for operators):

$$z = Z/Z_q, \quad p_z = P_z/P_q, \quad \eta = g\mu_B \left| \frac{\partial B_z}{\partial z} \right| / 2F_q, \quad (4)$$

where Z_q , P_q , and F_q are the ‘‘quants’’ of the coordinate, momentum, and force acting on the cantilever,

$$Z_q = \left(\frac{\hbar \omega_c}{k_c} \right)^{1/2}, \quad P_q = \hbar/Z_q, \quad F_q = k_c Z_q. \quad (5)$$

The variables Z and P_z are the ‘‘dimensional’’ coordinate and momentum of the cantilever tip, k_c is the cantilever ‘‘spring constant,’’ ω_c is its frequency, g is the ‘‘ g factor’’ of the spin (below we use $g=2$), $\partial B_z/\partial z$ is the magnetic-field gradient produced by the ferromagnetic particle at the spin location when the cantilever is in the equilibrium position with no spin ($z=0$). Note that the cantilever interacts with the z component of the spin, which is an integral of motion in our system. In the Hamiltonian (3), we omitted the term $(g\mu_B B_0/\hbar\omega_c)\hat{S}_z$, where B_0 is the magnetic field on the spin when the cantilever is at the origin ($z=0$). This term may be eliminated ‘‘physically’’ (by application of a uniform exter-

nal field of magnitude B_0 in the negative z direction) or ‘‘mathematically’’ (by transferring to the system of coordinates rotating with the frequency $g\mu_B B_0/\hbar$).

The master equation describes the evolution of the density matrix of the system interacting with the environment (see, for example, Refs. [5–8]). We are taking into account the interaction of the cantilever with its environment, and ignore the direct interaction between the spin and the environment, assuming that the spin relaxation and decoherence times are large enough. The effect of the environment depends on its ‘‘spectral density,’’ i.e., the density of environmental oscillators at a given frequency. Probably, the simplest model of the environment is the ‘‘ohmic’’ model, where the spectral density is proportional to the frequency ω for $\omega < \Omega$, where Ω is the cutoff frequency for the environment. A master equation for the non-ohmic environment has been derived in Ref. [8]. For the ohmic model, the simplest master equation has been obtained in Ref. [5]. This equation is valid in the ‘‘high-temperature limit’’ $k_B T \gg \hbar\Omega$. The master equation derived in Ref. [6] is valid for arbitrary temperature. As pointed out in Ref. [8], both master equations derived in Refs. [5,6] fail at times shorter than or close to $\hbar/k_B T$.

Note that quantum effects in nanomechanical oscillators have been studied previously (see, for example, Ref. [9]). However, to the best of our knowledge, the exact solution of the master equation for the spin-cantilever system has never been obtained.

We are going to consider the gedanken experiment discussed in Ref. [1]. Suppose that initially ($t=0$) the spin is in a superposition of the two states with the z projection of the spin $S_z=1/2$ and $S_z=-1/2$. These two states of the spin correspond to two different equilibrium positions of the cantilever tip. Thus, the cantilever (without decoherence) would transform into a MSCS: two simultaneous equilibrium positions. Certainly, decoherence will destroy this state. The master equation describes both the appearance of the MSCS and its destruction due to decoherence.

Following Ref. [1], we consider the ultrathin cantilever reported in Ref. [10]. It has the spring constant $k_c=6.5 \times 10^{-6}$ N/m, the frequency $\omega_c/2\pi=1.7$ kHz, and the quality factor $Q=6700$. The ferromagnetic particle on the cantilever tip is taken to be a sphere of radius $R=15$ nm at a distance 5 nm from the paramagnetic atom. (Below we consider conditions for increasing the distance between the cantilever and spin.) For this case, the static displacement of the cantilever tip due to its interaction with the single spin exceeds the thermal vibrations of the cantilever for temperatures

$$T < T_{max} = \frac{(\mu_B \partial B_z / \partial z)^2}{k_B k_c} \approx 1.7 \text{ mK}. \quad (6)$$

In our gedanken experiment for the temperature $T \gg \hbar\omega_c/k_B \approx 8 \times 10^{-8}$ K, we can use the simplest high-temperature limit in the ohmic model.

The master equation in the high-temperature limit can be written in the form [5]

$$\frac{\partial \rho_{s,s'}}{\partial \tau} = \left[\frac{i}{2}(\partial_{zz} - \partial_{z'z'}) - \frac{i}{2}(z^2 - z'^2) - \frac{1}{2}\beta(z - z')(\partial_z - \partial_{z'}) - D\beta(z - z')^2 - 2i\eta(z's' - zs) \right] \rho_{s,s'}. \quad (7)$$

Here, s and s' take values $\pm 1/2$ (we use s instead of S_z), $\tau = \omega_c t$, $\beta = 1/Q$, and $D = k_B T / \hbar \omega_c$. Using new coordinates

$$r = z - z', \quad R = \frac{1}{2}(z + z'), \quad (8)$$

Eq. (7) can be written as

$$\frac{\partial \rho_{s,s'}(R, r, \tau)}{\partial \tau} = \{i\partial_{Rr} - iRr - \beta r \partial_r - D\beta r^2 - i\eta[(2R - r)s' - (2R + r)s]\} \rho_{s,s'}(R, r, \tau). \quad (9)$$

Performing a Fourier transformation of this equation with respect to the variable R , one obtains, after rearrangements,

$$\frac{\partial \hat{\rho}_{s,s'}}{\partial \tau} + (\beta r - k) \frac{\partial \hat{\rho}_{s,s'}}{\partial r} + [r + 2\eta(s' - s)] \frac{\partial \hat{\rho}_{s,s'}}{\partial k} = [-D\beta r^2 + i\eta r(s' + s)] \hat{\rho}_{s,s'}, \quad (10)$$

where

$$\hat{\rho}_{s,s'}(k, r, \tau) = \int_{-\infty}^{+\infty} e^{ikR} \rho_{s,s'}(R, r, \tau) dR.$$

We can study separately the spin diagonal case ($s = s'$) and the off-diagonal case ($s \neq s'$). For $s' = s$ (up-up or down-down spins), we have the following equation:

$$\frac{\partial \hat{\rho}_{s,s}}{\partial \tau} + (\beta r - k) \frac{\partial \hat{\rho}_{s,s}}{\partial r} + r \frac{\partial \hat{\rho}_{s,s}}{\partial k} = (-D\beta r^2 + 2i\eta r s) \hat{\rho}_{s,s}, \quad (11)$$

and for $s' \neq s$ (up-down or down-up spins),

$$\frac{\partial \hat{\rho}_{s,-s}}{\partial \tau} + (\beta r - k) \frac{\partial \hat{\rho}_{s,-s}}{\partial r} + (r + 4\eta s) \frac{\partial \hat{\rho}_{s,-s}}{\partial k} = -D\beta r^2 \hat{\rho}_{s,-s}. \quad (12)$$

We will derive the exact solution of the master equation (7) for the case when the spin is ‘‘prepared’’ initially in the superposition of two states with $s = 1/2$ and $s = -1/2$, while the cantilever tip is in the quasiclassical coherent state

$$\psi(z, s, 0) = \frac{1}{(\pi)^{1/4}} \exp[ip_0 z - (z - z_0)^2 / 2] \otimes \begin{pmatrix} a \\ b \end{pmatrix}, \quad (13)$$

where the amplitudes a and b correspond to the values of $s = 1/2$ and $s = -1/2$, respectively. The corresponding density matrix can be written as

$$\rho_{ss'}(z, z', 0) = \psi(z, s, 0) \otimes \psi^\dagger(z', s', 0). \quad (14)$$

Note that we consider an ensemble of spin-cantilever systems with the same initial state. This implies that the experimenter can detect the position and momentum of a point on the cantilever tip with quantum limit accuracy $(\delta p_z)^2 (\delta z)^2 = 1/4$. (In our gedanken experiment, this corresponds to an uncertainty of 300 fm for position and 300 nm/s for velocity.) Based on the master equation, we can predict the average position of the cantilever tip for its given initial state, depending on the spin state. If the double uncertainty of the position is smaller than the separation between two possible average positions, the cantilever tip will measure the state of the spin.

After the Fourier transformation, the ‘‘cantilever part’’ of the density matrix is represented by

$$\hat{\rho}_{s,s'}(k, r, 0) \propto \exp[ip_0 r + ikz_0 - r^2/4 - k^2/4]. \quad (15)$$

IV. SOLUTION FOR SPIN DIAGONAL MATRIX ELEMENTS

The equations for the characteristics of Eq. (11) are

$$d\tau = \frac{dr}{\beta r - k} = \frac{dk}{r} = \frac{d\hat{\rho}_{s,s'}}{(-D\beta r^2 + 2i\eta sr)\hat{\rho}_{ss}}, \quad (16)$$

or, explicitly

$$\begin{aligned} \frac{dr}{d\tau} &= \beta r - k, \\ \frac{dk}{d\tau} &= r, \end{aligned} \quad (17)$$

$$\frac{d\hat{\rho}_{s,s'}}{d\tau} = (-D\beta r^2 + 2i\eta sr)\hat{\rho}_{s,s'}.$$

From the first two equations in Eq. (17), one obtains

$$\frac{d^2 k}{d\tau^2} - \beta \frac{dk}{d\tau} + k = 0,$$

which has the following general solution:

$$k = e^{\beta\tau/2} (c_1 \cos \theta\tau + c_2 \sin \theta\tau), \quad (18)$$

where $\theta = \sqrt{1 - \beta^2/4}$. (Here we are considering the case $\beta < 2$ so θ is a real number. The case $\beta > 2$ can also be solved analytically.) Using the second equation in Eq. (17), one obtains

$$r = e^{\beta\tau/2} \left[\left(\frac{\beta}{2} \cos \theta\tau - \theta \sin \theta\tau \right) c_1 + \left(\frac{\beta}{2} \sin \theta\tau + \theta \cos \theta\tau \right) c_2 \right]. \quad (19)$$

Inverting Eqs. (18) and (19) as a function of c_1 and c_2 , one obtains the characteristic curves

$$c_1 = e^{-\beta\tau/2} (q_1 k + q_2 r) \quad (20)$$

$$c_2 = e^{-\beta\tau/2}(p_1 k + p_2 r), \quad (21)$$

where the time-dependent constants q_1 , q_2 , p_1 , and p_2 have been defined as

$$q_1 = \frac{1}{\theta} \left(\frac{\beta}{2} \sin \theta\tau + \theta \cos \theta\tau \right),$$

$$q_2 = -\frac{1}{\theta} \sin \theta\tau,$$

$$p_1 = \frac{1}{\theta} \left(-\frac{\beta}{2} \cos \theta\tau + \theta \sin \theta\tau \right), \quad (22)$$

$$p_2 = \frac{1}{\theta} \cos \theta\tau.$$

Substituting Eq. (19) into the third equation of Eq. (17) and integrating in time, one obtains

$$\hat{\rho}_{s,s}(k, r, \tau) \propto Q(c_1, c_2) \exp[i2\eta s(c_1 g_1 + c_2 g_2) - D\beta(c_1^2 f_1 + 2c_1 c_2 f_3 + c_2^2 f_2)], \quad (23)$$

where the functions f_i 's and g_i 's are defined as

$$f_1(\tau) = \frac{e^{\beta\tau}}{8} \left[\left(\beta + \frac{4\theta^2}{\beta} \right) + \beta \cos 2\theta\tau - 2\theta \sin 2\theta\tau \right],$$

$$f_2(\tau) = \frac{e^{\beta\tau}}{8} \left[\left(\beta + \frac{4\theta^2}{\beta} \right) - \beta \cos 2\theta\tau + 2\theta \sin 2\theta\tau \right],$$

$$f_3(\tau) = \frac{e^{\beta\tau}}{8} [2\theta \cos 2\theta\tau + \beta \sin 2\theta\tau], \quad (24)$$

$$g_1(\tau) = e^{\beta\tau/2} \cos \theta\tau,$$

$$g_2(\tau) = e^{\beta\tau/2} \sin \theta\tau.$$

The arbitrary function A which depends on the characteristics is determined by the initial density matrix $\hat{\rho}_{s,s}(k(0), r(0), 0)$,

$$A(c_1, c_2) = \hat{\rho}_{s,s}(c_1, \frac{1}{2}\beta c_1 + \theta c_2, 0) \exp[-2i\eta s(c_1 g_{10} + c_2 g_{20})] \exp[D\beta(c_1^2 f_{10} + 2c_1 c_2 f_{30} + c_2^2 f_{20})], \quad (25)$$

where $f_{i0} = f_i(0)$ and $g_{i0} = g_i(0)$. From the initial density matrix [Eq. (15)], we obtain

$$\hat{\rho}_{s,s}(k, r, 0) \propto \exp\{i[(\frac{1}{2}p_0\beta + z_0)c_1 + p_0\theta c_2]\} \times \exp\left\{-\left[\left(\frac{\beta^2}{16} + \frac{1}{4}\right)c_1^2 + \frac{\beta\theta}{4}c_1 c_2 + \frac{\theta^2}{4}c_2^2\right]\right\}. \quad (26)$$

Substituting Eqs. (25) and (26) into Eq. (23), one obtains

$$\hat{\rho}_{s,s}(k, r, \tau) \propto \exp\left\{i\left[\left(\frac{1}{2}p_0\beta + z_0 + 2\eta s G_1\right)c_1 + (p_0\theta + 2\eta s G_2)c_2\right]\right\} \exp\left\{-\left[\left(\frac{\beta^2}{16} + \frac{1}{4}\right)c_1^2 + \frac{\beta\theta}{4}c_1 c_2 + \frac{\theta^2}{4}c_2^2\right]\right\} \exp\{-D\beta(F_1 c_1^2 + 2c_1 c_2 F_3 + F_2 c_2^2)\}, \quad (27)$$

where F_i and G_i are defined as

$$F_i(\tau) = f_i(\tau) - f_{i0}, \quad G_i(\tau) = g_i(\tau) - g_{i0}.$$

Substituting in Eq. (27) the values of the characteristics as a function of k and r [Eqs. (20) and (21)], one obtains

$$\hat{\rho}_{ss}(k, r, \tau) \propto \exp[-r^2 C_1 + ir C_2 + (iB_2 - rB_1)k - \sigma_*^2 k^2], \quad (28)$$

where

$$\sigma_*^2 = e^{-\beta t} \left[\left(\frac{\beta^2}{16} + \frac{1}{4} \right) q_1^2 + \frac{\beta\theta}{4} q_1 p_1 + \frac{\theta^2}{4} p_1^2 + D\beta(F_1 q_1^2 + 2q_1 p_1 F_3 + F_2 p_1^2) \right], \quad (29)$$

$$B_1 = e^{-\beta t} \left\{ \left(\frac{\beta^2}{16} + \frac{1}{4} \right) 2q_1 q_2 + \frac{\beta\theta}{4} (q_1 p_2 + q_2 p_1) + \frac{\theta^2}{4} 2p_1 p_2 + 2D\beta[F_1 q_1 q_2 + (q_1 p_2 + q_2 p_1)F_3 + F_2 p_1 p_2] \right\}, \quad (30)$$

$$B_2(s) = e^{-\beta t/2} \left[\left(\frac{1}{2} p_0 \beta + z_0 + 2\eta s G_1 \right) q_1 + (p_0 \theta + 2\eta s G_2) p_1 \right], \quad (31)$$

$$C_1 = e^{-\beta t} \left[\left(\frac{\beta^2}{16} + \frac{1}{4} \right) q_2^2 + \frac{\beta\theta}{4} q_2 p_2 + \frac{\theta^2}{4} p_2^2 + D\beta(F_1 q_2^2 + 2q_2 p_2 F_3 + F_2 p_2^2) \right], \quad (32)$$

$$C_2(s) = e^{-\beta t/2} \left[\left(\frac{1}{2} p_0 \beta + z_0 + 2\eta s G_1 \right) q_2 + (p_0 \theta + 2\eta s G_2) p_2 \right]. \quad (33)$$

In Eqs. (31) and (33), the explicit dependence on s is presented. Performing the inverse Fourier transform, one obtains

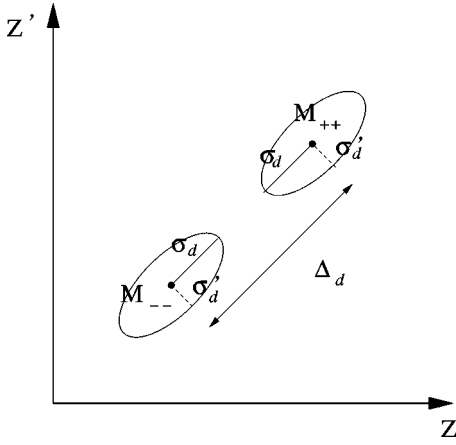


FIG. 2. Schematic view of the Gaussians representing the diagonal elements $|\rho_{-1/2,-1/2}|$ and $|\rho_{1/2,1/2}|$ (seen from the top) in the (z, z') plane. We show the centers M_{--} and M_{++} , the variances σ'_d (transverse) and σ_d (parallel), and the distance between diagonal centers Δ_d .

$$\begin{aligned} \rho_{1/2,1/2}(R, r, \tau) &= \frac{|a|^2}{2\sqrt{\pi}\sigma_*} \exp[-r^2 C_1 + ir C_2(1/2)] \\ &\quad \times \exp[-\{ -r B_1 + i B_2(1/2) - i R \}^2 / 4\sigma_*^2], \\ \rho_{-1/2,-1/2}(R, r, \tau) &= \frac{|b|^2}{2\sqrt{\pi}\sigma_*} \exp[-r^2 C_1 + ir C_2(-1/2)] \\ &\quad \times \exp[-\{ -r B_1 + i B_2(-1/2) - i R \}^2 / 4\sigma_*^2]. \end{aligned} \quad (34)$$

Equations (34) represent two squeezed Gaussians with modulus

$$\begin{aligned} |\rho_{1/2,1/2}(R, r, \tau)| &= \frac{|a|^2}{2\sqrt{\pi}\sigma_*} \exp[-r^2(C_1 - B_1^2/4\sigma_*^2)] \\ &\quad \times \exp[-\{ B_2(1/2) - R \}^2 / 4\sigma_*^2], \\ |\rho_{-1/2,-1/2}(R, r, \tau)| &= \frac{|b|^2}{2\sqrt{\pi}\sigma_*} \exp[-r^2(C_1 - B_1^2/4\sigma_*^2)] \\ &\quad \times \exp[-\{ B_2(-1/2) - R \}^2 / 4\sigma_*^2]. \end{aligned} \quad (35)$$

Figure 2 shows schematically two peaks (seen from the top as ellipses) corresponding to the two matrix elements $|\rho_{1/2,1/2}|$ and $|\rho_{-1/2,-1/2}|$. We denote the centers of the ellipses, which lie on the diagonal $z = z'$, by M_{++} and M_{--} , the semimajor axis by σ_d , the semiminor axis by σ'_d , and the distance between the centers by Δ_d . The $\rho_{1/2,1/2}^{max}$ is located at $M_{++} = (r=0, R=B_2(1/2))$ or $z = z' = B_2(1/2)$, while the $\rho_{-1/2,-1/2}^{max}$ is at $M_{--} = (r=0, R=B_2(-1/2))$ or $(z = z' = B_2(-1/2))$. The distance Δ_d is given by

$$\Delta_d = B_2(1/2) - B_2(-1/2). \quad (36)$$

From Eqs. (35), we obtain $\sigma_d = \sqrt{2}\sigma_*$ and

$$2\sigma_d'^2 = \frac{4\sigma_*^2}{4\sigma_*^2 C_1 - B_1^2}. \quad (37)$$

For a single-spin measurement, the two peaks corresponding to $\rho_{1/2,1/2}^{max}$ and $\rho_{-1/2,-1/2}^{max}$ must be well separated. It follows that the condition $\Delta_d > 2\sigma_d$ must be satisfied.

First, we consider the case $\beta\tau \gg 1$ or $\tau \gg Q/\omega_c$, where Q/ω_c is the time constant for the cantilever. In this case, we obtain two equilibrium positions for the cantilever, when the transient process is over. We have $\Delta_d = 2\eta$ and $\sigma_d = \sqrt{D}$. The value $\sigma_d = \sqrt{D}$ is the thermodynamical uncertainty in the cantilever position caused by the thermal noise. The two equilibrium positions can be distinguished if $\eta > \sqrt{D}$ or $T < F^2/k_B k_c$, where $F = \mu_B |\partial B_z / \partial z|$ is the magnetostatic force between the ferromagnetic particle and the paramagnetic atom. The last expression exactly coincides with formula (1).

Next, we consider the initial transient process after the instant ($t=0$) at which the paramagnetic spin has been transferred into the superpositional state. For $\beta\tau \ll 1$, we have

$$\Delta_d = 4\eta \sin^2 \frac{\tau}{2}, \quad \sigma_d = [1/2 + D\beta\tau - D\beta \cos \tau \sin^3 \tau]^{1/2}. \quad (38)$$

This expression for Δ_d describes the oscillating distance between the two peaks. It corresponds to initial vibrations of two classical oscillators near their equilibrium positions $z = \eta$ and $z = -\eta$. The distance between them is given by Δ_d . (For our gedanken experiment, the maximum value of Δ_d is 0.24 nm.) The formula for σ_d contains three terms. The first term $1/2$ corresponds to the quantum dispersion of the initial wave function. The second term $D\beta\tau$ describes the initial diffusion of an ensemble of oscillators. Formally, setting $\tau \sim 1/\beta$, we can estimate the final dispersion $\sigma_d = \sqrt{D}$, which corresponds to thermodynamical vibrations of the cantilever tip. The third term describes insignificant oscillations with small amplitude, $D\beta$.

Note that the condition for distinguishing the two cantilever positions at the beginning of the transient process is much less restrictive than the corresponding condition for the equilibrium positions at $\beta\tau \gg 1$. Indeed, after the first half period ($\tau = \pi$), we have $\Delta_d = 4\eta$ and $\sigma_d = (1/2 + \pi D\beta)^{1/2}$. Taking into account that $\beta \ll 1$, the condition for distinguishing the two positions, $\eta > (1/2 + \pi D\beta)^{1/2}$, is much easier than $\eta > \sqrt{D}$. In our gedanken experiment, the condition for distinguishing the two positions for the transient process is

$$T < T_{max} = \frac{4}{\pi} \frac{QF^2}{k_B k_c} = 14 \text{ K}, \quad (39)$$

compared with $T < T_{max} = 1.7 \text{ mK}$ for the static Stern-Gerlach effect. This estimate seems to be too optimistic. It is connected with the very small distance (5 nm) between the ferromagnetic particle and the paramagnetic atom. If we increase this distance to 50 nm, the temperature T_{max} drops

from 14 K to 1.1 mK. Unlike our gedanken experiment, a MFM experiment at the distance of 50 nm in the millikelvin region of temperatures seems to be a realistic proposal. (The MRFM experiments in the millikelvin region of temperatures have been already reported in Ref. [3].)

Note that expression (39) coincides exactly with our preliminary estimates (2).

The condition $\Delta_d > 2\sigma_d$ is satisfied for the first time at

$$\tau = \tau_0 \approx 2^{1/4} / \sqrt{\eta}. \quad (40)$$

This expression is valid if $\eta \gg 1$ and $\eta \gg (D\beta)^2 / \sqrt{8}$. For our gedanken experiment, we have $\eta = 144$, $D = 1.25 \times 10^7 T$ (T is the temperature in kelvin), $\beta = 1.5 \times 10^{-4}$, and $\tau_0 = 0.1$. Thus, the above conditions are both satisfied. The value of $t_0 = \omega_c \tau_0$ is $\approx 9.3 \mu\text{s}$.

V. SOLUTION FOR OFF-DIAGONAL SPIN MATRIX ELEMENTS

The equations for the characteristics are now given by

$$d\tau = \frac{dr}{\beta r - k} = \frac{dk}{r - 4\eta s} = \frac{d\hat{\rho}_{s,-s}}{-D\beta r^2 \hat{\rho}_{s,-s}}, \quad (41)$$

or

$$\begin{aligned} \frac{dr}{d\tau} &= \beta r - k, \\ \frac{dk}{d\tau} &= r - 4\eta s, \end{aligned} \quad (42)$$

$$\frac{d\hat{\rho}_{s,-s}}{d\tau} = -D\beta r^2 \hat{\rho}_{s,-s}.$$

The solutions of the first two equations of Eqs. (42) are

$$\begin{aligned} k &= e^{\beta\tau/2} (c_1 \cos \theta\tau + c_2 \sin \theta\tau) + 4\beta\eta s, \\ r &= e^{\beta\tau/2} \left[\left(\frac{\beta}{2} \cos \theta\tau - \theta \sin \theta\tau \right) c_1 + \left(\frac{\beta}{2} \sin \theta\tau + \theta \cos \theta\tau \right) c_2 \right] \\ &\quad + 4\eta s. \end{aligned} \quad (43)$$

Following the same steps as above, we obtain the following for the Fourier transform:

$$\begin{aligned} \hat{\rho}_{1/2,-1/2}(k,r,\tau) &\propto A(c_1, c_2) \exp\{-D\beta[f_1 c_1^2 + 2c_1 c_2 f_3 + f_2 c_2^2]\} \\ &\quad \times \exp\{-D\beta[4\eta(g_1 c_1 + g_2 c_2) + 4\eta^2 \tau]\}, \end{aligned} \quad (44)$$

where we fix $s = 1/2$ [changing sign of s corresponds to a change of sign of η , see Eq. (42), therefore the case $s = -1/2$ can be easily obtained]. The functions f_i and g_i have been defined as above, and c_1 and c_2 are new characteristic curves given by

$$\begin{aligned} c_1 &= e^{-\beta\tau/2} (q_1 k + q_2 r + \eta q_3), \\ c_2 &= e^{-\beta\tau/2} (p_1 k + p_2 r + \eta p_3). \end{aligned} \quad (45)$$

Here, q_1, q_2, p_1, p_2 are defined by Eqs. (22) and q_3, p_3 are given by

$$\begin{aligned} q_3 &= \frac{2}{\theta} \left[-\beta \left(\frac{\beta}{2} \sin \theta\tau + \theta \cos \theta\tau \right) + \sin \theta\tau \right], \\ p_3 &= \frac{2}{\theta} \left[\beta \left(\frac{\beta}{2} \cos \theta\tau - \theta \sin \theta\tau \right) - \cos \theta\tau \right]. \end{aligned} \quad (46)$$

With the same initial condition, Eq. (15), we can determine the function $A(c_1, c_2)$ and obtain

$$\begin{aligned} \hat{\rho}_{1/2,-1/2}(k,r,\tau) &\propto \hat{\rho}_{1/2,-1/2}(c_1 + 2\beta\eta, \frac{1}{2}\beta c_1 + \theta c_2 + 2\eta, 0) \\ &\quad \times \exp\{-D\beta[F_1 c_1^2 + 2c_1 c_2 F_3 + F_2 c_2^2 \\ &\quad + 4\eta(G_1 c_1 + G_2 c_2) + 4\eta^2 \tau]\}, \end{aligned} \quad (47)$$

where $F_i(\tau)$ and $G_i(\tau)$ are defined as above. By substituting the initial condition (15), we have

$$\begin{aligned} \hat{\rho}_{1/2,-1/2}(k,r,\tau) &\propto \exp[-r^2 C_{12} - r\eta C_{11} - \eta^2 C_{10} + irC_{21} + i\eta C_{20}] \\ &\quad \times \exp[(iB_{20} - rB_{11} - \eta B_{10})k - \sigma_*^2 k^2], \end{aligned} \quad (48)$$

where σ_* is given by Eq. (29) and

$$C_{12} = e^{-\beta\tau} \left[\left(\frac{\beta^2}{16} + \frac{1}{4} + D\beta F_1 \right) q_2^2 + \left(\frac{\beta\theta}{4} + 2D\beta F_3 \right) q_2 p_2 + \left(\frac{\theta^2}{4} + D\beta F_2 \right) p_2^2 \right],$$

$$\begin{aligned} C_{11} &= e^{-\beta\tau} \left[\left(\frac{\beta^2}{16} + \frac{1}{4} + D\beta F_1 \right) 2q_2 q_3 + \left(\frac{\beta\theta}{4} + 2D\beta F_3 \right) (q_2 p_3 + p_2 q_3) \right] + e^{-\beta\tau} \left[\left(\frac{\theta^2}{4} + D\beta F_2 \right) 2p_2 p_3 \right] \\ &\quad + 4e^{-\beta\tau/2} \left[\left(\frac{3\beta}{8} + D\beta G_1 \right) q_2 + \left(\frac{\theta}{4} + D\beta G_2 \right) p_2 \right], \end{aligned}$$

$$\begin{aligned}
C_{10} &= e^{-\beta\tau} \left[\left(\frac{\beta^2}{16} + \frac{1}{4} + D\beta F_1 \right) q_3^2 + \left(\frac{\beta\theta}{4} + 2D\beta F_3 \right) q_3 p_3 + \left(\frac{\theta^2}{4} + D\beta F_2 \right) p_3^2 \right] + 4e^{-\beta\tau/2} \left[\left(\frac{3\beta}{8} + D\beta G_1 \right) q_3 + \left(\frac{\theta}{4} + D\beta G_2 \right) p_3 \right] \\
&\quad + 4 \left(\frac{1}{4} + \frac{\beta^2}{4} + D\beta\tau \right), \\
C_{21} &= e^{-\beta\tau/2} \left[\left(\frac{p_0\beta}{2} + z_0 \right) q_2 + p_0\theta p_2 \right], \\
C_{20} &= e^{-\beta\tau/2} \left[\left(\frac{p_0\beta}{2} + z_0 \right) q_3 + p_0\theta p_3 \right] + 2(p_0 + z_0\beta), \\
B_{11} &= e^{-\beta\tau} \left[\left(\frac{\beta^2}{16} + \frac{1}{4} + D\beta F_1 \right) 2q_2q_1 + \left(\frac{\beta\theta}{4} + 2D\beta F_3 \right) (q_1p_2 + q_2p_1) \right] + e^{-\beta\tau} \left[\left(\frac{\theta^2}{4} + D\beta F_2 \right) 2p_2p_1 \right], \\
B_{10} &= e^{-\beta\tau} \left[\left(\frac{\beta^2}{16} + \frac{1}{4} + D\beta F_1 \right) 2q_3q_1 + \left(\frac{\beta\theta}{4} + 2D\beta F_3 \right) (q_1p_3 + q_3p_1) \right] + e^{-\beta\tau} \left[\left(\frac{\theta^2}{4} + D\beta F_2 \right) 2p_3p_1 \right] \\
&\quad + 4e^{-\beta\tau/2} \left[\left(\frac{3\beta}{8} + D\beta G_1 \right) q_1 + \left(\frac{\theta}{4} + D\beta G_2 \right) p_1 \right], \\
B_{20} &= e^{-\beta\tau/2} \left[\left(\frac{1}{2} p_0\beta + z_0 \right) q_1 + p_0\theta p_1 \right].
\end{aligned} \tag{49}$$

Performing the inverse Fourier transform and taking the modulus, we obtain

$$\begin{aligned}
|\rho_{1/2,-1/2}(R,r,\tau)| &= \frac{|ab^*|}{\sqrt{\pi\sigma_*}} e^{\xi\eta^2} e^{-(r+r_0\eta)^2/2\tilde{\sigma}^2} e^{-(B_{20}-R)^2/4\sigma_*^2}, \\
|\rho_{-1/2,1/2}(R,r,\tau)| &= \frac{|a^*b|}{\sqrt{\pi\sigma_*}} e^{\xi\eta^2} e^{-(r-r_0\eta)^2/2\tilde{\sigma}^2} e^{-(B_{20}-R)^2/4\sigma_*^2},
\end{aligned} \tag{50}$$

where

$$\begin{aligned}
\tilde{\sigma}^2 &= \frac{2\sigma_*^2}{4\sigma_*^2 C_{12} - B_{11}^2}, \\
r_0 &= \frac{2\sigma_*^2 C_{11} - B_{11} B_{10}}{4\sigma_*^2 C_{12} - B_{11}^2}, \\
\xi &= \frac{B_{10}^2}{4\sigma_*^2} - C_{10} - \frac{r_0^2}{2\tilde{\sigma}^2}.
\end{aligned} \tag{51}$$

The maxima are located at $(R=B_{20}, r=-\eta r_0)$ for $|\rho_{1/2,-1/2}|$ and at $(R=B_{20}, r=\eta r_0)$ for $|\rho_{-1/2,1/2}|$. In (z, z') coordinates, this corresponds to $M_{+-} = (z=B_{20}-\eta r_0/2, z'=B_{20}+\eta r_0/2)$ for $|\rho_{1/2,-1/2}|$ and $M_{-+} = (z=B_{20}+\eta r_0/2, z'=B_{20}-\eta r_0/2)$ for $|\rho_{-1/2,1/2}|$, so that the distance between them is given by $\Delta_{nd} = \sqrt{2}\eta|r_0|$. Next, we consider the quadratic form $(r \pm r_0\eta)/2\tilde{\sigma}^2 + (B_{20}-R)^2/4\sigma_*^2$ in the (z, z') plane. Straightforward calculations show that this is an ellipse

whose semiaxes are, respectively, given by $\tilde{\sigma}$ (across the diagonal) and $2\sqrt{2}\sigma_*$ (along the diagonal). The centers of the peaks M_{+-}, M_{-+} are symmetric with respect to the diagonal line $z=z'$.

The most remarkable difference compared with the diagonal case is the presence of irreversible decoherence. Indeed, the heights of the peaks are exponentially reduced in time by the damping factor $\sim \exp(-4\eta^2 D\beta\tau)$. This, in turn, defines a characteristic time scale of decoherence: $\tau_d = 1/4\eta^2 D\beta$. This formula exactly coincides with the expression derived in Ref. [1], based on a semiquantitative analysis. The value of τ_d is very small. In our gedanken experiment $\tau_d \approx 60$ ps at the temperature $T=1$ mK.

At time $\tau = \tau_0$, when two diagonal peaks are clearly separated, the damping factor is $4\eta^2 D\beta\tau_0$. We expect to observe the coherence between the two peaks macroscopic quantum superposition if this factor is not more than one unit. Thus, using the expression for τ_0 from Eq. (40), we can estimate the condition for the quantum coherence as $D\beta\eta^{3/2} < 1$, or

$$T < T_{max} = \frac{Q}{k_B} \frac{(\hbar\omega_c)^{7/4} k_c^{3/4}}{F^{3/2}}. \tag{52}$$

For our gedanken experiment the value of T_{max} is approximately 3×10^{-7} K.

Now, we will check the validity of our estimate for the parameters chosen for our gedanken experiment. Our solution is valid if $\eta \gg (D\beta)^2/\sqrt{8}$. Setting $T=T_{max}$ or $D\beta\eta^{3/2} = 1$, we obtain $\eta^4 \gg 1/\sqrt{8}$, which is definitely true, assuming $\eta \gg 1$. Next, the condition of the validity of the high tem-

perature approximation is $D \gg 1$. For $T = T_{max}$, it follows that $\eta^{3/2} \ll Q$. This inequality is roughly satisfied ($\eta^{3/2} = 1700$, $Q = 6700$). Finally, as we mentioned in the Introduction, the master equation fails at times $t \leq \hbar/k_B T$. Thus, the time considered, $\tau_0 = 2^{1/4}/\sqrt{\eta}$, must be much greater than $1/D$, which is definitely wrong. Thus, our condition (52) for the creation of the macroscopic quantum superposition is not justified for the parameters considered.

Next, we discuss at what values of the parameters a macroscopic quantum superposition can be generated. First, we emphasize the qualitative difference between the following two conditions: (1) the condition for distinguishing two positions of the cantilever and (2) The condition for distinguishing two positions of the cantilever and the coherence between these two positions. The first condition is relatively simple: $T < T_{max} = F^2/k_B k_c$ for equilibrium positions ($\tau \gg Q$) and $T < T_{max} = 4QF^2/\pi k_B k_c$ for $\tau = \pi$. The obvious way to increase T_{max} is by decreasing the spring constant k_c or increasing the magneto-static force F . For $\tau = \pi$, one additional way is to increase the quality factor Q . Condition (2) for generating an macroscopic quantum superposition can be satisfied at temperature $T < T_{max} = \hbar^{7/4} Q k_c^{13/8} / k_B F^{3/2} m^{7/8}$, where m is the effective mass of the cantilever, $m = k_c / \omega_c^2$. At $T = T_{max}$, the macroscopic quantum superposition will be generated if we satisfy the inequalities $1 \ll \eta^2 \ll Q$, or

$$1 \ll \frac{mF^2}{\hbar k_c^{3/2}} \ll Q. \quad (53)$$

One can see that the regime considered in our paper does not allow free manipulation of any parameter but Q . Increasing Q , we can satisfy the second inequality and, at the same time, increase T_{max} . In our gedanken experiment, the tenfold increase of Q ($Q = 67000$) provides the validity of the right-hand inequality in Eq. (53) and increases T_{max} to 3μ K.

VI. CONCLUSION

We have shown that the maximum temperature for a single-spin measurement in MFM can be increased by a factor of Q if one utilizes the initial transient process instead of the static displacement of the cantilever tip. We have obtained an exact analytical solution of the master equation, which describes the Q -times magnification of the maximum temperature. In addition, we have found the conditions for generation of macroscopic Schrödinger cat state in MFM.

ACKNOWLEDGMENTS

The work of G.P.B. was supported by the U.S. Department of Energy (DOE) under Contract No. W-7405-ENG-36. G.P.B. and V.I.T. thank the National Security Agency (NSA), the Advanced Research and Development Activity (ARDA), and DARPA (MOSAIC) for partial support.

-
- [1] G.P. Berman, G.D. Doolen, P.C. Hammel, and V.I. Tsifrinovich, *Phys. Rev. A* **65**, 032311 (2002).
 [2] J.A. Sidles, *Rev. Mod. Phys.* **67**, 249 (1995).
 [3] H.C. Mamin and D. Rugar, *Appl. Phys. Lett.* **79**, 3358 (2001).
 [4] B.C. Stipe, H.J. Mamin, C.S. Yannoni, T.D. Stowe, T.W. Kenny, and D. Rugar, *Phys. Rev. Lett.* **87**, 277602 (2001).
 [5] A.O. Caldeira and A.T. Leggett, *Physica A* **121**, 587 (1983);
Ann. Phys. (N.Y.) **149**, 374 (1983).
 [6] W.G. Unruh and W.H. Zurek, *Phys. Rev. D* **40**, 1071 (1989).
 [7] A. Venugopalan, *Phys. Rev. A* **56**, 4307 (1997).
 [8] B.L. Hu, J.P. Paz, and Y. Zhang, *Phys. Rev. D* **45**, 2843 (1992).
 [9] W.H. Zurek, *Phys. Today* **44**(10), 36 (1991).
 [10] T.D. Stowe, K. Yasumura, T.W. Kenny, D. Botkin, K. Wago, and D. Rugar, *Appl. Phys. Lett.* **71**, 288 (1997).